Supporting Information

Silicon Nanoparticles with a Polymer-Derived Carbon Shell for Improved Lithium-Ion Batteries: Investigation into Volume Expansion, Gas Evolution, and Particle Fracture

Alexander Schiele,[†] Ben Breitung,[*,†,‡] Andrey Mazilkin,[†,‡,§] Simon Schweidler,[†] Jürgen Janek,[†,∥] Simon Gumbel,[⊥] Sven Fleischmann,[⊥] Ewelina Burakowska-Meise,[⊥] Heino Sommer,[⊥] and Torsten Brezesinski[*,†]

[†]Battery and Electrochemistry Laboratory and [‡]Institute of Nanotechnology, Karlsruhe Institute of Technology, Hermann-von-Helmholtz-Platz 1, 76344 Eggenstein-Leopoldshafen, Germany

[§]Institute of Solid State Physics, Russian Academy of Sciences, Ac. Ossipyan str. 2, 142432 Chernogolovka, Russia

[∥]Institute of Physical Chemistry & Center for Materials Science, Justus-Liebig-University Giessen, Heinrich-Buff-Ring 17, 35392 Giessen, Germany

[⊥]BASF SE, Carl-Bosch-Strasse 38, 67056 Ludwigshafen, Germany

E-mail: ben.breitung@kit.edu, torsten.brezesinski@kit.edu

Table of Contents

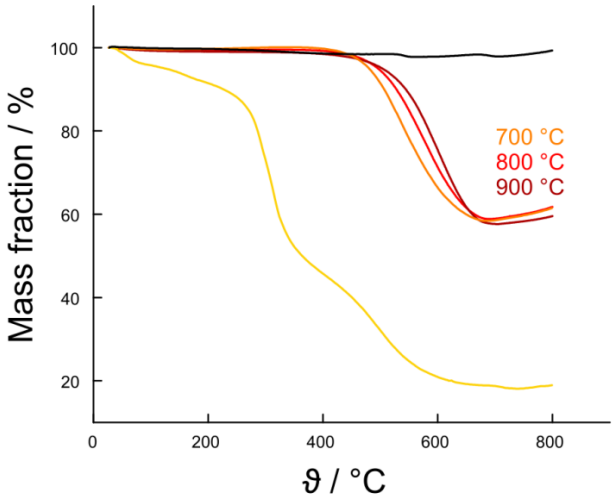

Figure S1. TGA in air of pristine Si particles (black), Si/C composite particles after different treatments (orange, red, and dark red), and Si-based precursor material (yellow). The heating rate was 5 °C min^{-1}.

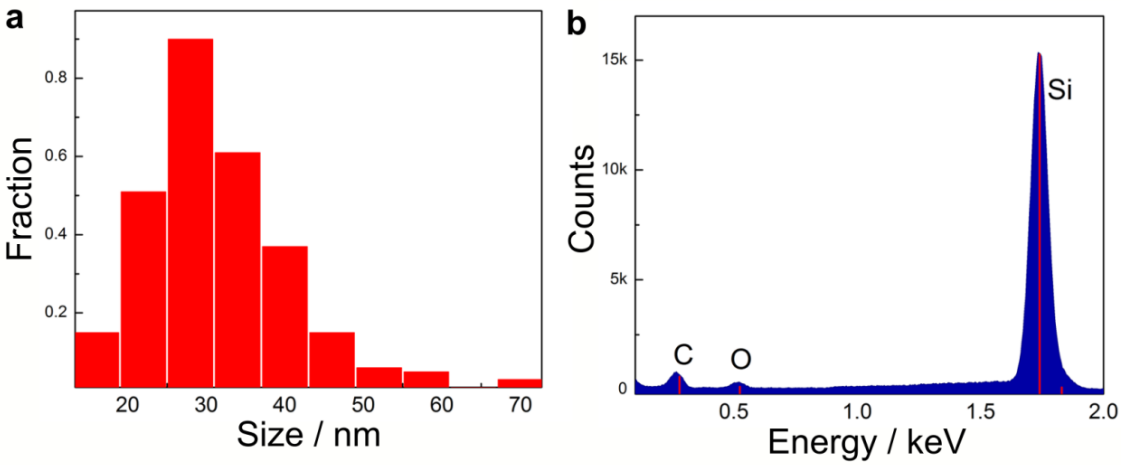

Figure S2. (a) Particle size distribution determined by counting ≈300 particles from TEM images. The average particle size is (28 ± 9) nm. (b) Integrated EDX spectrum revealing an Si:C:O mass ratio of 87.5:10:2.5.

The D and G bands from Raman spectroscopy for Si/C composite particles after different treatments are depicted in panel (a) of **Figure S3**. According to Cançado *et al.*, the crystallite size, L_a, of nanographitic systems can be calculated as follows:[1]

$$L_a = (2.4 \times 10^{-10})\lambda_l^4 \left(\frac{I_D}{I_G}\right)^{-1}$$

where λ_l is the wavelength of the excitation laser (here, 532 nm) and I_D and I_G represent the integrated intensities (areas) of the D and G bands, respectively. The Raman spectra were fitted (green curve), and the contributions of the D (blue curve) and G bands (dark yellow) were determined individually.

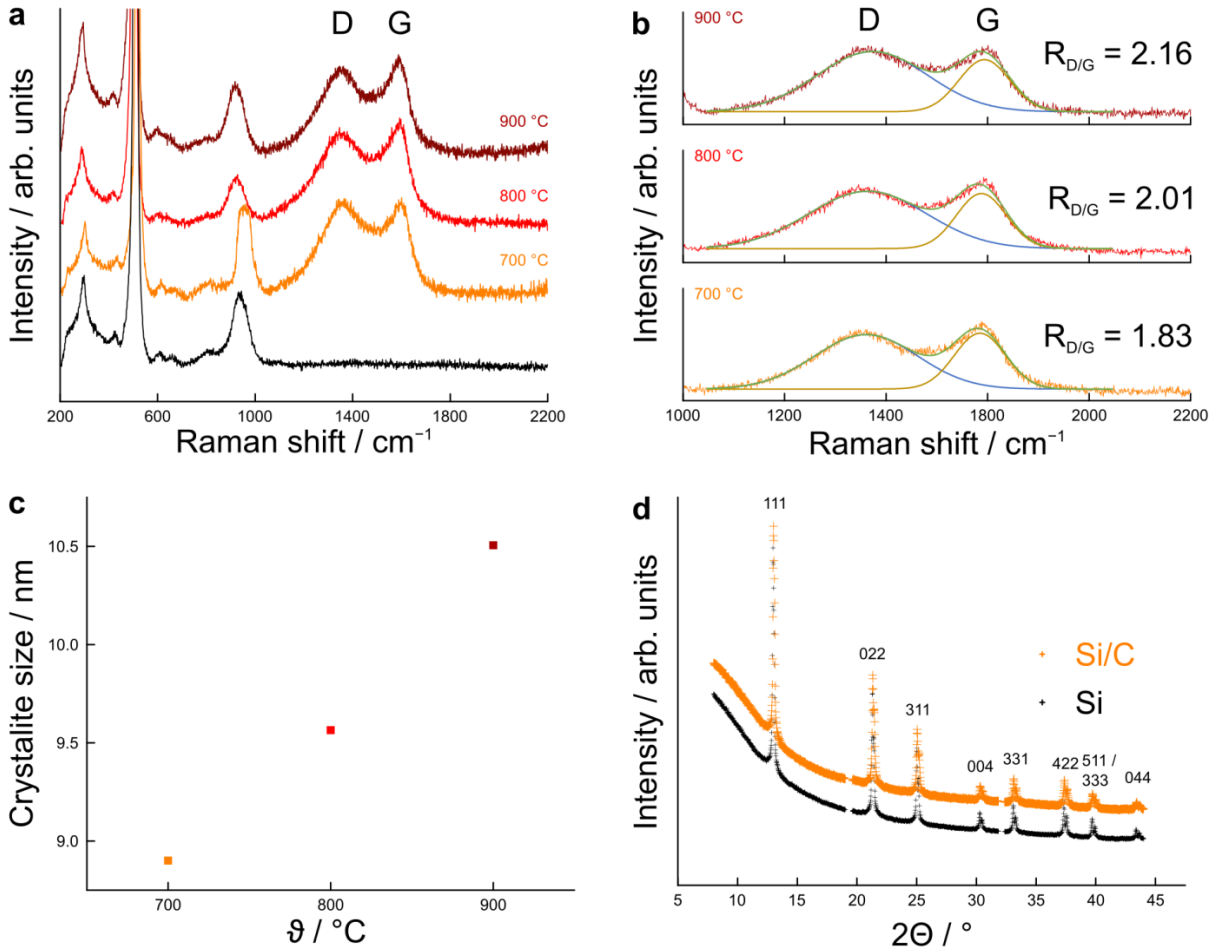

Figure S3. (a) Raman spectrum of pristine Si particles (black) and Si/C composite particles after different treatments (orange, red, and dark red). (b) Fitting of the D and G bands of carbon with Gaussian profiles. The ratio of the integrated D and G band intensities is indicated. (c) Lateral extent of graphene layers with increasing carbonization temperature according to Cançado *et al*.[1] (d) XRD pattern of pristine Si particles (black) and Si/C composite particles (orange).

Table S1. Detailed cycling protocol of half-cells using either pristine Si particles or Si/C composite particles as the anode active material. The CV step at the cut-off potential was limited by residual current (1/10th of the nominal current).

#	Process	Cut-off potential	Rate	Mode	Number of cycles
1	Lithiation	10 mV	C/20	CCCV	2
2	Delithiation	1000 mV	C/20	CCCV	
3	Lithiation	30 mV	C/10	CCCV	3
4	Delithiation	600 mV	C/10	CCCV	
5	Lithiation	30 mV	C/2	CCCV	5
6	Delithiation	600 mV	C/2	CCCV	
7	Lithiation	30 mV	C/2	CCCV	2
8	Delithiation	600 mV	1C	CC	
9	Lithiation	30 mV	C/2	CCCV	2
10	Delithiation	600 mV	3C	CC	
11	Lithiation	30 mV	C/2	CCCV	1
12	Delithiation	600 mV	C/10	CC	
13	Lithiation	30 mV	C/2	CCCV	25
14	Delithiation	600 mV	C/2	CCCV	

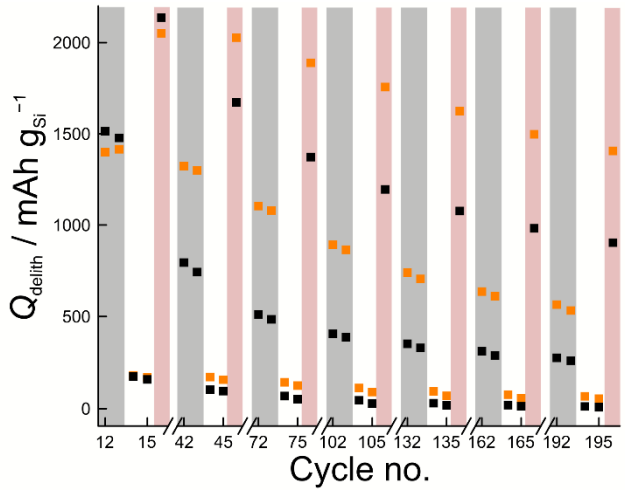

Figure S4. Analysis of the rate performance of half-cells with FEC-based electrolyte using pristine Si particles (black) or Si/C composite particles (orange). Note that specific delithiation capacities at rates of 1C (gray), 3C (white), and C/10 (pink) are shown.

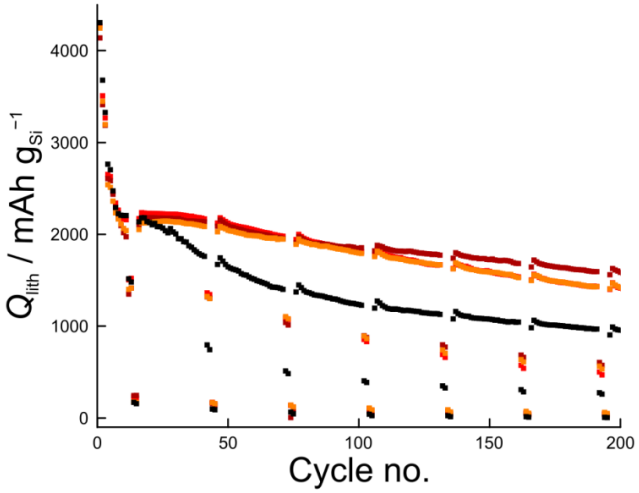

Figure S5. Specific lithiation capacities of pristine Si particles (black) and Si/C composite particles after heating at 700 (orange), 800 (red), and 900 °C (dark red). The areal loading was 1.2-1.3 mg_{Si} cm^{-2}.

For *in situ* pressure measurements, ("zero-strain") LTO was used as the counter electrode.[2] Prelithiation of LTO was done at a rate of C/10, with a CV step at 1.0 V vs. Li^+/Li until the current dropped to C/100. The specific lithiation capacity achieved was 170.5 mAh g_{LTO}^{-1}, which is in good agreement with the theoretical one. The cell using prelithiated LTO cathode and Si/C composite-containing anode was cycled at C/10 in the potential range between 1.6 and 0.9 V.

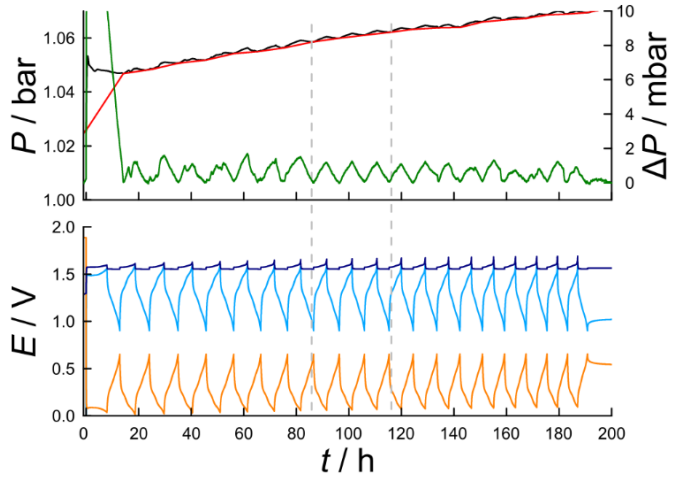

Figure S6. *In situ* pressure measurement conducted on a cell with LP57 electrolyte using prelithiated LTO and Si/C composite particles as cathode and anode, respectively. The top panel shows the pressure evolution (black), the irreversible contributions due to gassing (red), and the reversible contributions (green) due to volume expansion/contraction of Si during cycling. The cycles used for determination of the volume changes are denoted by dashed gray lines. The bottom panel depicts the cell potential (light blue), the potential of the LTO electrode (dark blue), and the Si electrode potential (orange) at C/10 rate.

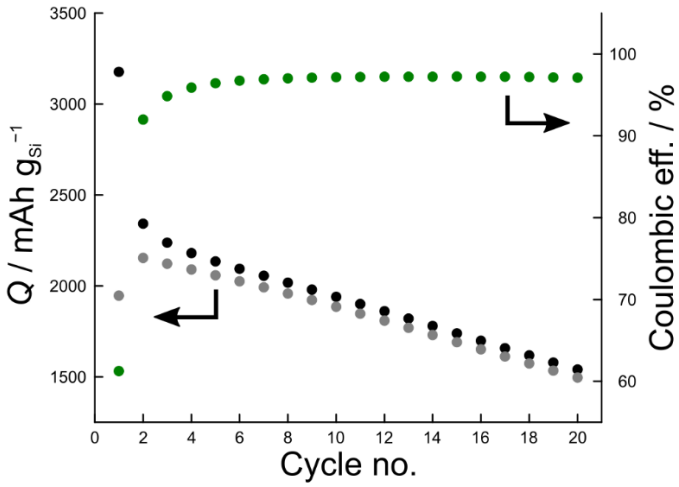

Figure S7. Specific lithiation (black) and delithiation (gray) capacities and the corresponding Coulombic efficiencies (green) of the cell in **Figure S6** used for determination of the volume changes.

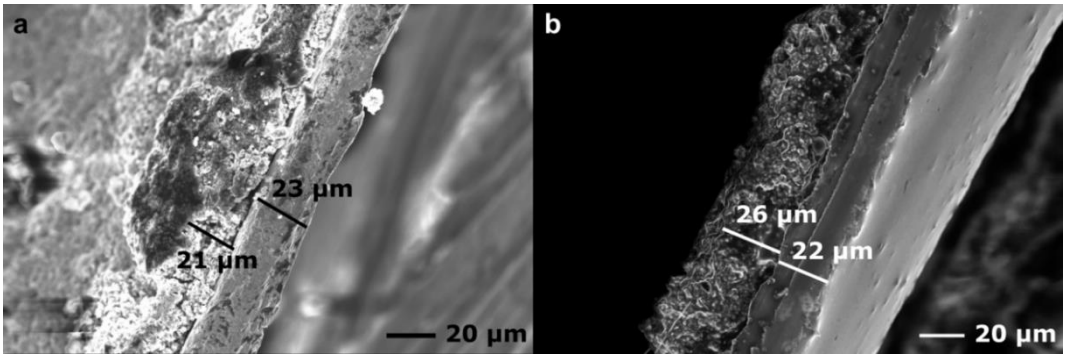

Figure S8. Cross-sectional SEM images of Si/C composite-containing electrodes before (a) and after 20 cycles (b). The thickness of both the Cu current collector and the active electrode layer is indicated. The cycled electrode was washed with 1 mL DMC to remove electrolyte residues prior to imaging.

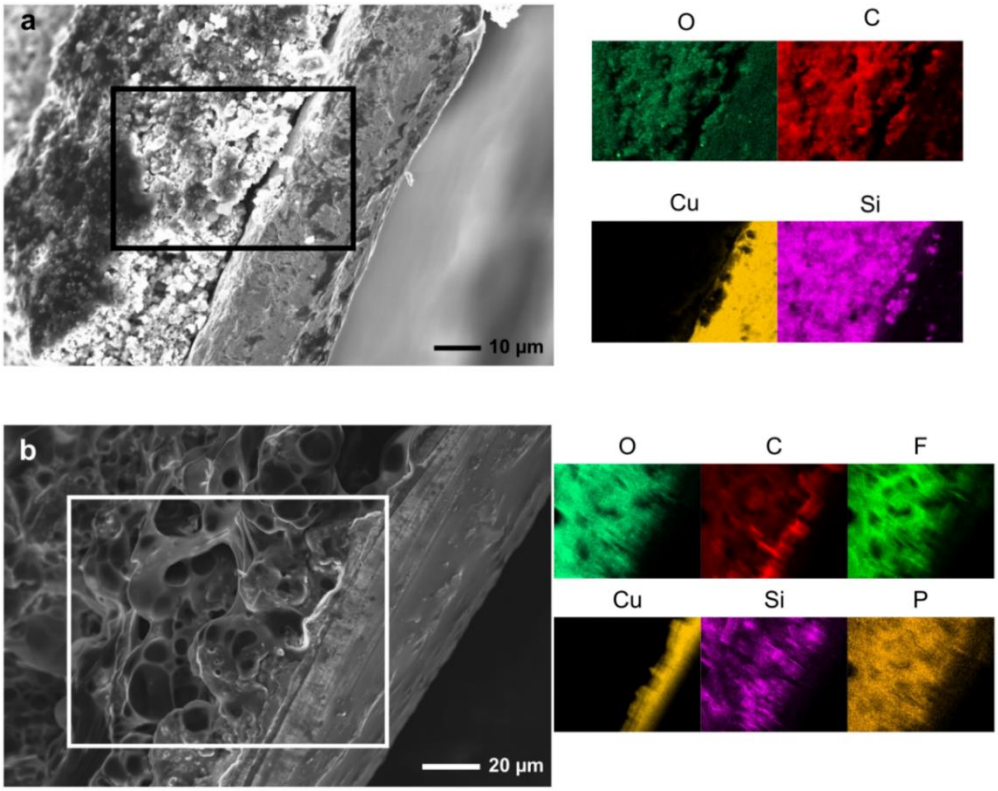

Figure S9. Cross-sectional SEM images of Si/C composite-containing electrodes before (a) and after 20 cycles (b) and EDX maps of O, C, Cu, and Si and O, C, F, Cu, Si, and P for the area denoted by the black and white box, respectively. The cycled electrode was washed with 1 mL DMC to remove electrolyte residues prior to imaging and mapping analysis.

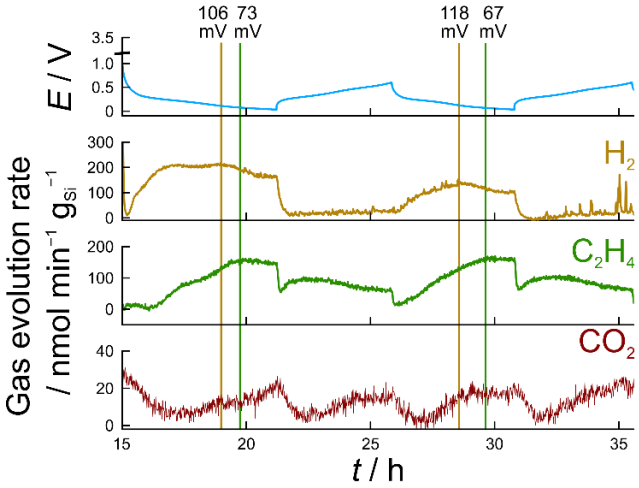

Figure S10. DEMS measurement of a half-cell with LP57 electrolyte using the Si/C composite particles. Note that only the 2nd and 3rd cycles at C/10 are shown. The cell potential (light blue) is correlated to the evolution rates of H_2 (yellow), C_2H_4 (green), and CO_2 (red). Maxima in the H_2 and C_2H_4 evolution rates are denoted by vertical lines.

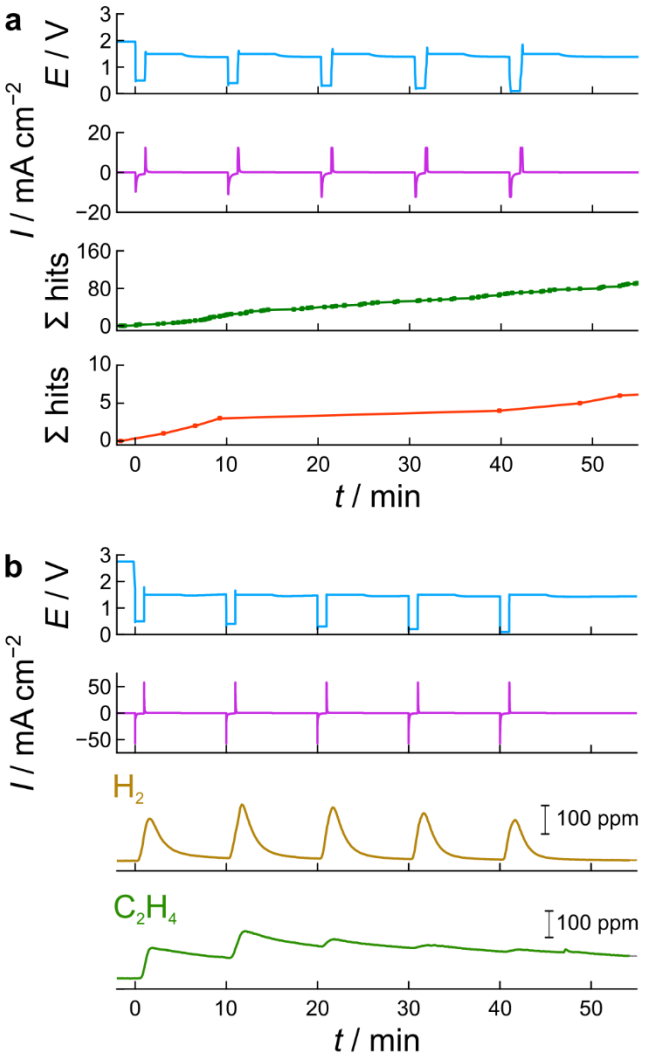

Figure S11. Chronoamperometric measurements on Super C65 carbon/Li cells with LP57 electrolyte analyzed via AE (a) and DEMS (b). The cell potential (light blue) after OCV period was controlled as follows: 500 mV, 400 mV, 300 mV, 200 mV, and 100 mV each for 1 min. The upper potential was set to 1.5 V for 4 min, followed by an OCV period of 5 min between the individual steps. The current response is shown in violet. (a) Cumulated unfiltered (dark green) and filtered hits (red). Each detected event is denoted by a solid square. (b) Evolution characteristics of H_2 (yellow) and C_2H_4 (green).

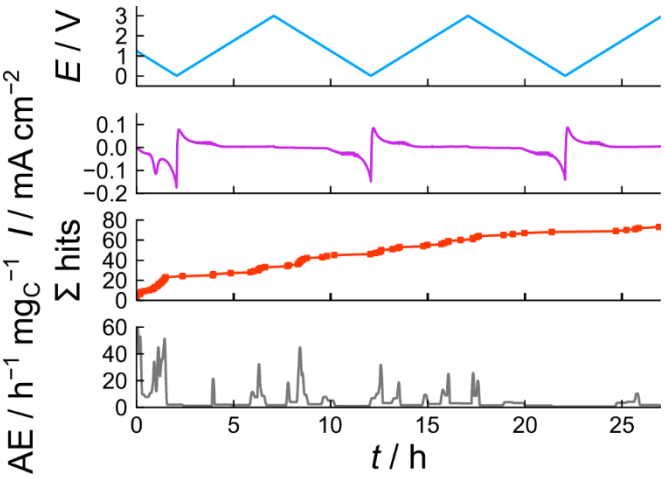

Figure S12. Cyclic voltammetry and the corresponding AE data of a Super C65 carbon/Li cell using LP57 electrolyte. The potential range was set between 3.0 V and 10 mV (light blue) and the sweep rate was 0.58 V h^{-1}. The current response (violet) as well as the cumulated filtered hits (red) and AE hit rate (gray) are shown.

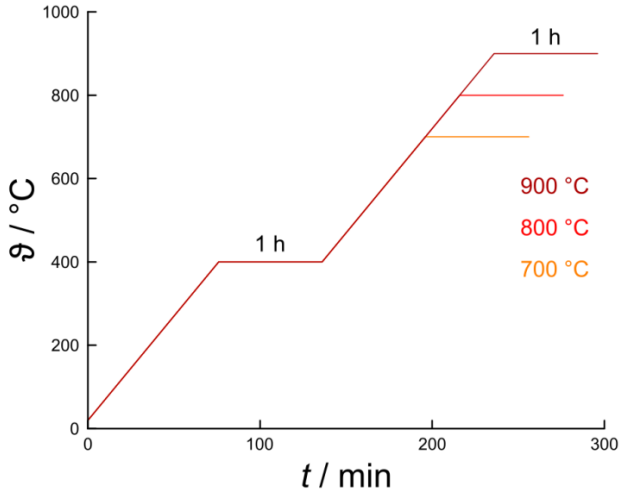

Figure S13. Temperature profile of the heating process to produce Si/C composite particles. The heating rate was 5 °C min^{-1} with dwell time of 1 h at 400 °C and 700, 800, or 900 °C. The final material was naturally cooled to room temperature.

Appendix S1

The volume change of the Si electrode, ΔV_{Si}, was calculated according to:[3]

$$\Delta V_{\%} = \frac{\Delta V_{\mathrm{Si}}}{V_{\mathrm{Si}}} = \frac{\Delta V_{\mathrm{Si}} \varrho_{\mathrm{Si}}}{m_{\mathrm{Si}}}$$

with ϱ_{Si} = 2.336 g cm^{-3} and

$$\Delta V_{\mathrm{Si}} = V_{\mathrm{Cell}} \left(\frac{\Delta P}{P_0(\mathrm{t}) + \Delta P} \right)$$

ΔP is the reversible change in pressure (green curve in **Figure S6**) and P_0(t) is the irreversible increase in pressure (red curve in **Figure S6**). In order to determine the cell volume, V_{Cell}, a custom setup was used. The general procedure is described elsewhere.[4]

References

(1) Caṇado, L. G.; Takai, K.; Enoki, T.; Endo, M.; Kim, Y. A.; Mizusaki, H.; Jorio, A.; Coelho, L. N.; Magalhães-Paniago, R.; Pimenta, M. A. General Equation for the Determination of the Crystallite Size L_a of Nanographite by Raman Spectroscopy. *Appl. Phys. Lett.* **2006**, *88*, 163106.

(2) Ohzuku, T.; Ueda, A.; Yamamoto, N. Zero-Strain Insertion Material of $Li[Li_{1/3}Ti_{5/3}]O_4$ for Rechargeable Lithium Cells. *J. Electrochem. Soc.* **1995**, *142*, 1431–1435.

(3) Schweidler, S.; de Biasi, L.; Schiele, A.; Hartmann, P.; Brezesinski, T.; Janek, J. Volume Changes of Graphite Anodes Revisited: A Combined *Operando* X-ray Diffraction and *In Situ* Pressure Analysis Study. *J. Phys. Chem. C* **2018**, *122*, 8829–8835.

(4) Schiele, A.; Hatsukade, T.; Berkes, B. B.; Hartmann, P.; Brezesinski, T.; Janek, J. High-Throughput In Situ Pressure Analysis of Lithium-Ion Batteries. *Anal. Chem.* **2017**, *89*, 8122–8128.